

Performance of the Hobby-Eberly telescope and facility instruments*

Gary. J. Hill^{a†}, Phillip J. MacQueen^a,
Lawrence W. Ramsey^b & Matthew D. Shetrone^c

^aMcDonald Observatory, University of Texas at Austin, 1 University Station C1402, Austin, TX 78712-0259, USA

^bDepartment of Astronomy and Astrophysics, Pennsylvania State University, University Park, PA 16802, USA

^cHobby-Eberly telescope, University of Texas at Austin, 1 University Station C1403, Austin, TX 78712-0259, USA

ABSTRACT

The Hobby-Eberly Telescope (HET) is a revolutionary large telescope of 9.2 meter aperture, located in West Texas at McDonald Observatory. The HET operates with a fixed segmented primary and has a tracker which moves the four-mirror corrector and prime focus instrument package to track the sidereal and non-sidereal motions of objects. The HET has been taking science data for five years, but the image quality and primary mirror stability have been far from specifications. Work over the past two years has improved performance significantly, and demonstrated site-seeing limited images of 0.8 arcsec., showing that the telescope will meet all specifications. The performance of the HET is discussed in detail.

The first phase of HET instrumentation includes three facility instruments: the Low Resolution Spectrograph (LRS), the Medium Resolution Spectrograph (MRS), and High Resolution Spectrograph (HRS). The current status of the instruments is described. Upcoming near infrared capabilities for the LRS and MRS are also discussed.

Keywords: Telescopes: Hobby-Eberly Telescope, Astronomical instrumentation: Spectrographs

1. INTRODUCTION: OVERVIEW OF THE HET AND INSTRUMENTS

The HET^{1,2,3} is a unique telescope with an 11 m hexagonal-shaped spherical mirror made of 91 1 m hexagonal segments that sits at a fixed zenith angle of 35°. It can be moved in azimuth to access about 70% of the sky visible at McDonald Observatory. HET is a collaboration of the University of Texas at Austin, Pennsylvania State University, Stanford University, Georg-August-Universität, Göttingen, and Ludwig-Maximilians-Universität, Munich. The pupil is 9.2 m in diameter, and sweeps over the primary mirror as the x-y tracker follows objects for between 40 minutes (in the south at $\delta = -10.3^\circ$) and 2.8 hours (in the north at $\delta = +71.6^\circ$). The maximum track time per night is 5 hours and occurs at $+63^\circ$. Detailed descriptions of the HET and its commissioning can be found in refs 1-5. Currently the HET is operating with its first two facility instruments, the Marcario Low resolution Spectrograph (LRS)⁶⁻⁸, which rides in the Prime Focus Instrument Package (PFIP) on the tracker, allowing it to image as well as take spectra, and the fiber-fed High Resolution Spectrograph (HRS)^{3,9} installed in the basement spectrograph room under the telescope internal to the pier. The Medium Resolution Spectrograph (MRS)^{10,11} is undergoing commissioning and is already taking science queue data. The HRS and MRS are fed by fibers from the fiber instrument feed (FIF)¹⁰ that is part of the PFIP.

The primary mirror has a radius of curvature of 26164 mm, and a 4-mirror double-Gregorian type corrector is designed to produce images with FWHM < 0.6 arcsec in the absence of seeing, over a 4 arcmin (50 mm) diameter

* The Hobby – Eberly Telescope is operated by McDonald Observatory on behalf of the University of Texas at Austin, the Pennsylvania State University, Stanford University, Ludwig-Maximilians-Universität München, and Georg-August-Universität, Göttingen

† G.J.H.: E-mail: hill@astro.as.utexas.edu

science field of view^{8,12}. A moving baffle is installed at a pupil on the fourth mirror of the corrector and will block stray light as the pupil tracks off the primary. Another mirror folds the light-path towards the LRS, for a total of six reflections to reach the LRS slit. The FIF is fed directly without a further reflection.

2. HET UPGRADE PROJECT AND CURRENT PERFORMANCE

The HET is a prototype for a new breed of cost-effective large telescopes. As such, it is essentially a test-bed for engineering and operations concepts designed to minimize cost while maintaining performance. In particular, the primary mirror¹³, based on a steel truss, and the tracker¹⁴ were key to realizing the project for the initial modest cost of \$16M. Initial performance of the HET was not, however, to specification in the areas of image quality and primary mirror stability⁷. Subsequent completion of the telescope to improve image quality, as described below, will bring the total expenditure to about \$20M, still a very modest price for a large telescope³. The price paid for this low cost is that HET and its sister Southern African Large Telescope (SALT)¹⁵ are the most complex telescopes in existence, requiring constant realignment of the optics during a track in order to maintain image quality. Since last reported⁵, we have achieved site-seeing limited images as described below, and are now confident that HET will perform to or surpass its initial specifications.

In conjunction with image quality improvements at HET, we now have a three-year baseline of site seeing measurements recorded by Direct Image Motion Monitors. The median zenith seeing has been 1.0 arcsec FWHM with the best images being 0.7 arcsec or better 9% of the time. The summer seeing is better than in winter (0.9 versus 1.3 arcsec). At the 35 degree zenith distance of the HET, this translates to a median of 1.13 arcsec, and minimum of 0.8 arcsec FWHM.

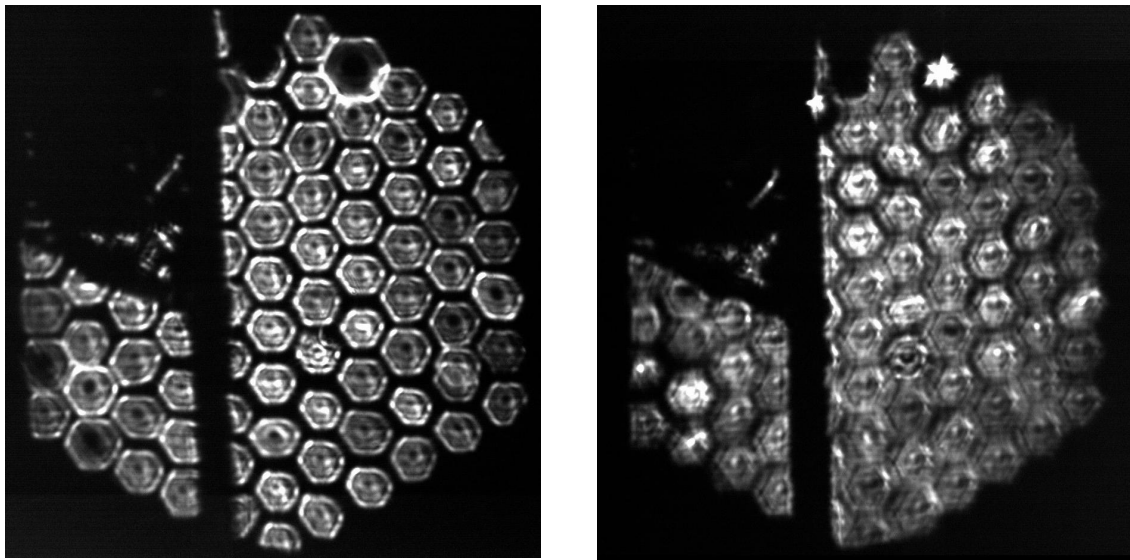


Figure 1: Example of extra-focal imaging of the full primary mirror of HET with HEFI. The shadow of the tracker beam and instrument payload is blocking the top left of the image. The segments have the expected appearance, with bright edges, but some show distortions symptomatic of astigmatism (e.g. middle of the far right edge) or of incorrect focal length (top right). These aberrations are due to problems with the segment mounts but make a negligible contribution to current image quality (see text)

The image quality delivered by the HET depends on (a) the accuracy of the primary mirror alignment (stack), (b) the stability of the primary mirror to changes in temperature and gravity, (c) dome seeing, (d) accuracy of the motions of the tracker, and (e) the figure and internal alignment of the corrector. In early operations, typical images delivered by the telescope were 2.5-3.0 arcsec FWHM⁴. Since then, we have undertaken a series of projects designed to understand the poor image quality of the HET and to correct the problem, with the goal of achieving the HET image quality

specification of 0.9 arcsec FWHM in the best expected site-seeing of 0.7 arcsec. As will be discussed below, we have met this specification. Here we describe the process of understanding and improving the performance of the HET. Refer to ref 3 for further details.

2.1 Primary Mirror Image Quality

2.1.1 The Mirror Alignment Recovery System (MARS)

The polarizing shearing interferometer system (CCAS) delivered with the HET to effect the alignment (stacking) of the 91 mirror segments to form a single image, proved to be unusable in practice. After a significant evaluation and commissioning effort¹⁶, we determined that the capture range of the CCAS instrument was inadequate. As a replacement, we elected to build a Shack-Hartmann system, to produce an image from each mirror that could be aligned with a fiducial spot. This system, called MARS¹⁷, has been operational since October 2001 and has dramatically improved the quality of the primary mirror alignment. At this point, we are able to align the mirror segments to 0.2 arcsec rms (projected on the sky), and alignment now has a negligible effect on the delivered image quality. Operational efficiency has also been improved with the MARS system, with typical restacks taking only about 10 minutes under normal conditions.

2.1.2 The Segment Alignment Maintenance System (SAMS)

The SAMS project corrected a significant shortfall in the HET primary mirror (PM) stability¹⁸. We were experiencing significant degradation in the quality of the alignment in typically only an hour, primarily due to temperature driven motions of the mirror segments on the PM truss. NASA Marshall Space Flight Center and Blueline Engineering were contracted to produce an edge sensor system for the HET PM utilizing small inductive sensors. The project started in November 1999, and SAMS has been in operation since January 2002. SAMS uses inductive sensors, which have sensitivity to temperature, and we found it necessary to calibrate each sensor in order to improve the temperature stability of the system. For temperature changes within ± 1.5 degrees of the temperature at which the PM was aligned, the degradation is now acceptable. For larger temperature excursions, we are forced to realign the PM with MARS. In practice, two alignments per night are typically required, so the overhead is well within the HET specification that <10% of observing time be used for alignment. The improvement in the overall performance of the HET from the installation of SAMS has, been quite dramatic. Maintaining the global radius of curvature (GROC) of the PM within ± 0.3 mm of 26,164 mm is an important aspect of HET performance. GROC is controlled by SAMS through a combination of temperature sensing and mirror-gap sensing. Temperature changes drive the ROC of the steel mirror truss and cause the mean gap size

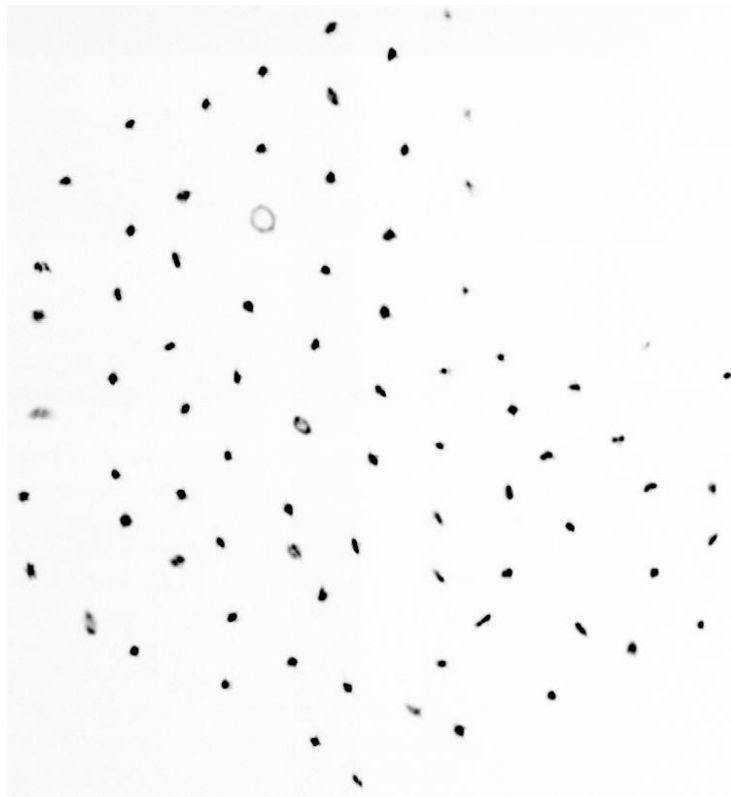


Figure 2: An image at center of curvature of a “Hex-burst” of the primary mirror, showing segments with astigmatism and a number with significant defocus. The separation between segment images is ~ 3 arcsec. The combined image of these segments has 0.4 arcsec FWHM

Temperature changes drive the ROC of the steel mirror truss and cause the mean gap size

between mirrors to change. Gap size is sensed as a common mode by the SAMS, and corrections are applied to the GROC. We believe that with proper calibration this scheme will work, but currently drift in GROC is an operational difficulty that still has to be overcome.

2.1.3 the HET Extra-Focal Imager (HEFI)

In order to evaluate the performance of the PM both in initial stack quality and in long-term stability, it was necessary to develop a extra-focal imaging instrument. The values for stability and stack quality reported here were derived with this instrument. HEFI consists of a CCD camera on a precise stage to allow images to be obtained at the center of curvature (CoC) of the PM and at precise distances either side of it. This system then allows several aspects of the PM performance to be evaluated:

- Image quality of the stacked mirror at CoC
- Image quality of the individual segments at CoC
- Surface figure of the individual segments with EF imaging and Hartmann mask imaging
- Surface figure of the entire primary mirror
- Accuracy of the mirror stack with Hartmann imaging, with a mask on each mirror segment

Figure 1 shows an example of EF imaging of the full primary mirror. The images either side of focus reveal some segments to be astigmatic at about 1.0 arcsec. This is not atypical as shown in Figure 2, which is taken at the CoC with the stack burst out into a hexagonal pattern. At first glance, these segment figures and images seem poor, but in reality they combine to form an image from the primary of 0.4 arcsec. FWHM (0.5 arcsec. EE(50%)), which meets the specifications. As a result, the PM is making a negligible contribution to even the best images delivered by the telescope. It appears that problems with the hubs of the individual mirror segment mounts are responsible for the aberrations seen in some of the segment images, and the mounts are being re-engineered. When this process is complete, the PM image quality will far exceed the initially required specification.

2.2 The Dome Environment and Seeing

Dome seeing was a major component of the poor image quality delivered initially by HET⁴. The original ventilation concept used a down-draft fan system similar to that on the Keck telescopes to draw ambient air in through the dome aperture. The system proved inadequate to the task of flushing the dome under typical conditions encountered in West Texas. In particular, we could improve the seeing significantly by changing from looking down-wind to looking into the wind, and it became obvious that significant perforations of the HET enclosure would be required to prevent stagnant air conditions. The Dome Ventilation System (DVS)¹⁹ consists of a series of 15 louver panels modeled after those on the Mayall 4 m at KPNO. The louvers were installed in 2002, and the image quality was seen to steadily improve during installation. The success of the system can be demonstrated on many nights by simply closing the louvers and watching the seeing degrade to 2.5 arcsec! In addition, we have applied adhesive aluminum strips to cover the dome and reduce its emissivity. This prevents super-cooling of the dome skin at night that creates currents of falling cold air, which are as bad as rising warm air for seeing.

Significant remaining heat sources on the tracker have been eliminated by ducting the heat away, and the pupil of the telescope no longer shows any local sources of convection. Dome seeing, as measured with a DIMM from inside the dome and at the CoC of the primary mirror, is now negligible, usually.

2.3 The Corrector and Mount Model

Another aspect of image quality that is unique to the HET design, is the effect of the tracker position on the image. The HET is a complex opto-mechanical system with no natural axes: everything is time-dependent. A trajectory for the tracker is loaded into the tracker control computer from the telescope control computer. This trajectory controls the x-y position of the tracker, and the six hexapod legs and rotation axis that manipulate the payload. In order to track an object accurately, the tracker payload must be maintained on the focal sphere of the spherical primary mirror, and must be pointed accurately perpendicular to it. The tracker¹⁴ has six axes: x, y, focus (z), tip (θ), tilt (ϕ), rotation (ρ). In order to maintain image quality during a track, the "mount model" needs to accurately maintain the 4-mirror corrector in the FPIP perpendicular to the PM within 25 seconds of arc, and in focus to within 10 μm . The tracker is actively guided in

x, y only, and the other axes run open-loop. During a track, the PFIP rotates (up to $\pm 19.4^\circ$ in the north) to maintain a fixed PA on the sky.

Having established that the primary mirror is meeting specifications and is stable over time, we were in a position to evaluate the image quality of the 4-mirror corrector and the accuracy of the mount-model. Hartmann mask imaging at the prime focus of HET revealed significant residual astigmatism in the images under typical track conditions, and the remaining 1.3 arcsec image quality floor could have been due to any of the following issues:

- Poor figure on one or more the mirrors in the corrector
- Poor alignment or stability of the alignment of the mirrors in the corrector
- Poor tracking of the required focal surface relative to the primary mirror during the track

We started by investigating the third possibility, because demonstration that good images could be obtained under carefully controlled engineering conditions would vindicate the quality of the corrector figure and alignment. Tip and tilt errors of the corrector with respect to the primary mirror result in astigmatic images, as revealed by the Hartmann mask imaging. With the HET tracking, the tip and tilt of the corrector were adjusted manually, while observing an out of focus image on the acquisition camera at bent prime focus. This “visual wavefront sensing” allowed astigmatism to be eliminated and an offset was introduced into the mount model to maintain that tip and tilt. The telescope was then brought back into focus, and image quality of 0.8 arcsec FWHM was achieved, with site seeing of 0.7 arcsec. FWHM recorded by the DIMM (Figure 3). This image quality was maintained for the rest of the track (20 minutes), and could be obtained, repeatably, under similar test conditions. It became immediately clear that the optical system of the HET meets specifications and that the remaining problems lie in the inaccuracy of the tracking mount model. In retrospect, it should not be surprising that an open-loop mount model proved inadequate for maintaining the alignment of this complex optical system.

We are in the process of enabling closed-loop feedback on the tip/tilt and focus of the tracker with respect to the primary mirror using a distance measuring interferometer and a laser autocollimator. This is the system adopted by the SALT¹⁵. In the meantime, the mount model has been improved significantly and the HET now quite often delivers images of ~ 1.0 arcsec. FWHM, under normal science conditions. Ultimately, however, we wish to move to a wavefront sensor feedback for the alignment of the tracker since this deals directly with what we care about. We can prototype such a system with the current corrector, but its application would be severely limited for most science by the limited field of view of the current corrector. We are planning to upgrade the HET with a much wider field corrector (20 arcminutes field diameter), and this upgrade is driven significantly by the need for bright wavefront sensing stars within the field of view for all observations.

2.4 Throughput of the HET

The HET optical design includes five reflections to reach prime focus (six to reach the LRS). Denton Vacuum FSS-99TM enhanced silver was chosen, initially, which has high reflectivity at wavelengths above 400 nm, and is better than bare aluminum for $\lambda > 380$ nm. Accounting for central obstruction, the pellicle guider, and the atmosphere, the predicted on-axis efficiency was 54% at 600 nm for prime focus and 52% for the light delivered to the LRS. We have encountered significant degradation of these coatings in practice, and Denton Vacuum re-coated the corrector mirrors in mid-2000. The mirrors continued to degrade, so the corrector mirrors were recoated in 2003 with a high durability broad-bandpass LLNL reflective coating²⁰. These surfaces are performing well. The primary mirror segment coatings are still the original ones, and have degraded to $\sim 45\%$ reflectivity at V. As a result, the on-sky throughput of the HET is now about 23% at the LRS input, and 25% at the fiber-feed. In addition, the coatings are scattering significantly, and the background measured during dark time is a magnitude brighter than recorded at the other telescopes at McDonald. This scattered light is in the pupil of the HET and cannot be baffled. The combination of low reflectivity and high scattering is degrading the performance of the telescope by a magnitude in sensitivity for background-limited observations. We have started recoating the segments with bare aluminum, and should complete the process by the end of 2004. In the longer term we are developing a coating facility for HET that will allow more complex coatings to be applied to the segments in the future. An upside of the change in coatings is that the telescope will have good UV throughput, opening up new scientific avenues for second generation instruments.

2.5 The Next Steps

To summarize, the HET is delivering median images of 1.5-1.7 arcsec FWHM, with the best images during normal science operations in the 1.0 to 1.2 arcsec range. These images are dominated by alignment errors during the track, rather than by primary mirror alignment, de-stack, or seeing. Under engineering conditions sub-arcsecond site-seeing limited images can be obtained, demonstrating that the HET optics meet specification. Installation of metrology equipment to provide direct feedback about the position of the tracker with respect to the primary mirror will improve

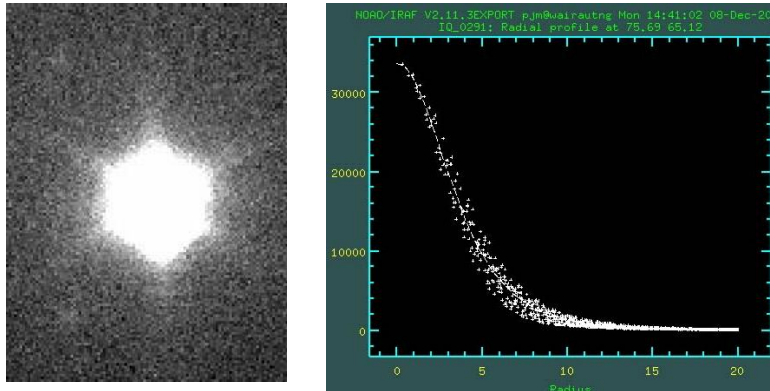


Figure 3: Examples of on-sky image quality obtained under engineering conditions. The image on the left obtained at bent prime focus with the acquisition camera has 0.82 arcsec FWHM, 1.0 arcsec EE(50%), and good symmetry as shown by the radial plot. At the time of this observation the site seeing was recorded to be 0.7 arcsec FWHM, and the primary mirror stack was 0.44 arcsec FWHM

the alignment accuracy, and should be complete within a year. On the same timeframe, the primary mirror will be recoated with aluminum, and the HET should at that point be meeting or surpassing its initial specifications.

3. THE FACILITY INSTRUMENTS

Currently, the HET is making queue-scheduled observations with the Marcario Low Resolution Spectrograph (LRS) and the High Resolution Spectrograph (HRS). The Medium Resolution Spectrograph (MRS) is being commissioned and is in use for limited queue-scheduled science. We concentrate on instrument development that has occurred in the last two years since the previous review⁵.

3.1 The Marcario Low Resolution Spectrograph

The LRS⁶⁻⁸ is a high-throughput grism spectrograph with three modes of operation: imaging, longslit, and multi-object. The field of view of the HET is 4 arcmin in diameter, and the LRS has a 13-slitlet Multi Object Spectroscopy (MOS) unit covering this field. The MOS unit²¹ is based on miniature components and is remotely configurable under computer control. All observing modes are now available in the HET queue. A series of longslits (1.0, 1.5, 2.0, 3.0, and 10.0 arcsec wide) may be selected, each 4-arcmin long. Typically, observations are obtained with the 2.0 arcsec wide slit due to the present imaging performance of the HET. A selection of 12 broad band and blocking filters are carried at any one time, along with two grisms.

The LRS mounts in a restricted space, as part of the PFIP, which rides on the HET tracker. The principal consequence of the tight space and weight constraints is to limit the range of configurations that may be carried by the LRS at any one time. The HET is queue-scheduled, so the limited configurations are factored into the queue-selection of projects executable on any given night. While it might be desirable to have all components available at any time, the overhead of calibrating a large number of possible configurations used on a given night does result in considerable inefficiency. We do not consider this limitation to be a significant drawback given the overall operating philosophy for the HET.

The LRS entered early science operations on October 6, 1999. Over the ensuing period we have made significant gains in improving the operational efficiency of the telescope, and the LRS has undergone one significant over-hall. The major improvement since the last update has been in the guider optics. The difficulty in tracking focus open loop discussed above, led us to replace the simple re-imaging system with improved optics based on a Canon 200 mm f/1.8 lens and a large commercial doublet. The result is much better image quality, with the ability to sense focus changes and keep the tracker in focus for long exposures. The guider has recorded sub-arcsecond images. It has finally proven

possible to combine multiple observations of faint targets with LRS from different tracks and achieve the expected improvement in S/N ratio. Previously, the great variability in image quality delivered by the telescope prevented this. The only drawback of the new guider configuration is that the field of view is reduced to 2.6x2.6 arcmin², and some observations in sparse fields have difficulty acquiring a guidestar. The useful limiting guidestar magnitude is V~17.5. This situation should improve as the HET primary mirror coatings are replaced.

LRS now operates with three gratings: grism 1 is 300 l/mm covering 407 to 1170 nm at a resolving power R~600 with a 1 arcsec wide slit; grism 2 is 600 l/mm covering 426 – 730 nm at R~1300. Grism 1 covers more than one octave of wavelength, and is used with blocking filters GG385 or OG515 depending on which part of the wavelength range is needed. Grism 2 is also used with the GG385 blocking filter since the LRS has sensitivity down to 360 nm. We have deployed a new first-order grism (grism G3) based on a volume holographic grating (VHG)²¹. The wavelength coverage is 630 to 900 nm at R~2000 in first order. This grating has 700 fringes per mm and is used at a Bragg angle of 11.5 degrees. This angle of incidence (and diffraction) is achieved by sandwiching the grating between two identical prisms of SF57 with AR coated outer faces. The throughput with this grism at 700 nm equals the peak with grism 1 at 550 nm at about 11% with the degraded HET primary mirror coatings. As the primary is aluminized, the performance of LRS will improve markedly, particularly for background limited observations of faint objects, where the combination of poor reflectivity and high scattering of the degraded coatings is costing a magnitude of sensitivity. The best images recorded during setup observations with the LRS have had 1.0 arcsec FWHM (without intensive adjustment of the corrector orientation for best image quality). The median images are ~1.7 arcsec FWHM, however, so control of the tracking as discussed above will result in significant further improvement in the sensitivity of LRS.

3.2 The Medium Resolution Spectrograph

Table 1: Basic properties of the HET Medium Resolution Spectrograph

| Medium Resolution Spectrograph (MRS) | | |
|---|-----------------------------------|-----------------------------------|
| | Visible Beam | NIR Beam |
| Fiber Fed MOS: Maximum number of Objects | 9 | 5 |
| Wavelength range (nm) | | |
| <i>Typical</i> | 430-880 | 1000-1300 |
| <i>Blue Limit</i> | 380 | 900 |
| <i>Red limit</i> | 900 | 1350 |
| Resolution-slit product (R ϕ arc-sec) | 10,400 | 10,400 |
| Max. resolution | ~20,000 | 10,400 |
| Camera | dioptric F/1.2 | dioptric F/1.6 |
| Detectors | Two 2K x 4K, Marconi 15 μm pixels | 1k x1k HgCdTe Hawaii 18 μm pixels |
| Echelle | 79 or 110 g/mm, R2 | 31.6 g/mm, R2 |
| Crossdispersers (g/mm and wavelength of max. efficiency) | #1: 900 g/mm, 5150 nm | #1: 400 g/mm, 1200 nm |
| | #2: 600 g/mm, 650nm | #2 TBD |
| | #3: 1200 g/mm, 560 nm | |
| | #4: 220 g/mm, 590 nm | |

The HET Medium Resolution Spectrograph (MRS)^{10,11} is a versatile, fiber-fed echelle spectrograph. This instrument is designed for a wide range of scientific investigations and includes single-fiber inputs for the study of point-like sources, synthetic slits of fibers for long slit spectroscopy, 10 independently positionable probes for single or multi-object spectroscopy, and the potential for a fiber integral field unit (IFU). The MRS consists of two beams. Table 1 summarizes the basic properties of the MRS. The visible beam has wavelength coverage from 450 - 900 nm in a single exposure with resolving power between 5,000 and 20,000 depending on the fiber configuration selected. This beam also has capability in the ranges 380 - 950 nm by altering the angles of the cross-disperser gratings. A second beam operating in the near-infrared has coverage of 900 - 1300 nm in a single exposure with resolving power between 5,500 and 11,000. Both beams can be used simultaneously and are fed by the HET Fiber Instrument Feed (FIF) which is mounted at the prime focus of the telescope and positions the fibers feeding the MRS and the HRS. The MRS started commissioning summer 2002.

3.2.1 Fibers and the Fiber Instrument Feed

The fiber instrument feed (FIF)¹⁰ on the tracker provides the MRS with multiple fiber-feed options, including 9 multi-object probes and 30-arcsec. fiber longslits. It also provides a probe for the HRS. For reference, for MRS, a 2-arcsec diameter fiber gives a resolution of $R=5080$. Output slits in the instrument allow selection of higher resolving power, at the expense of light-loss. The fiber length to the basement spectrograph room is 35 m. Both red (low OH) and blue (high OH) optimized fibers are available in the bundle, since the fiber length is such that attenuation is significant in the blue for the red fibers and in the absorption bands for the blue fibers. The best fiber for a given observation is chosen by offsetting the appropriate probe in the FIF. Each probe is outfitted with a small coherent bundle feeding a CCD camera, and one probe has a larger field bundle for coarse acquisition.

3.2.2 Layout and Optical Design of the MRS

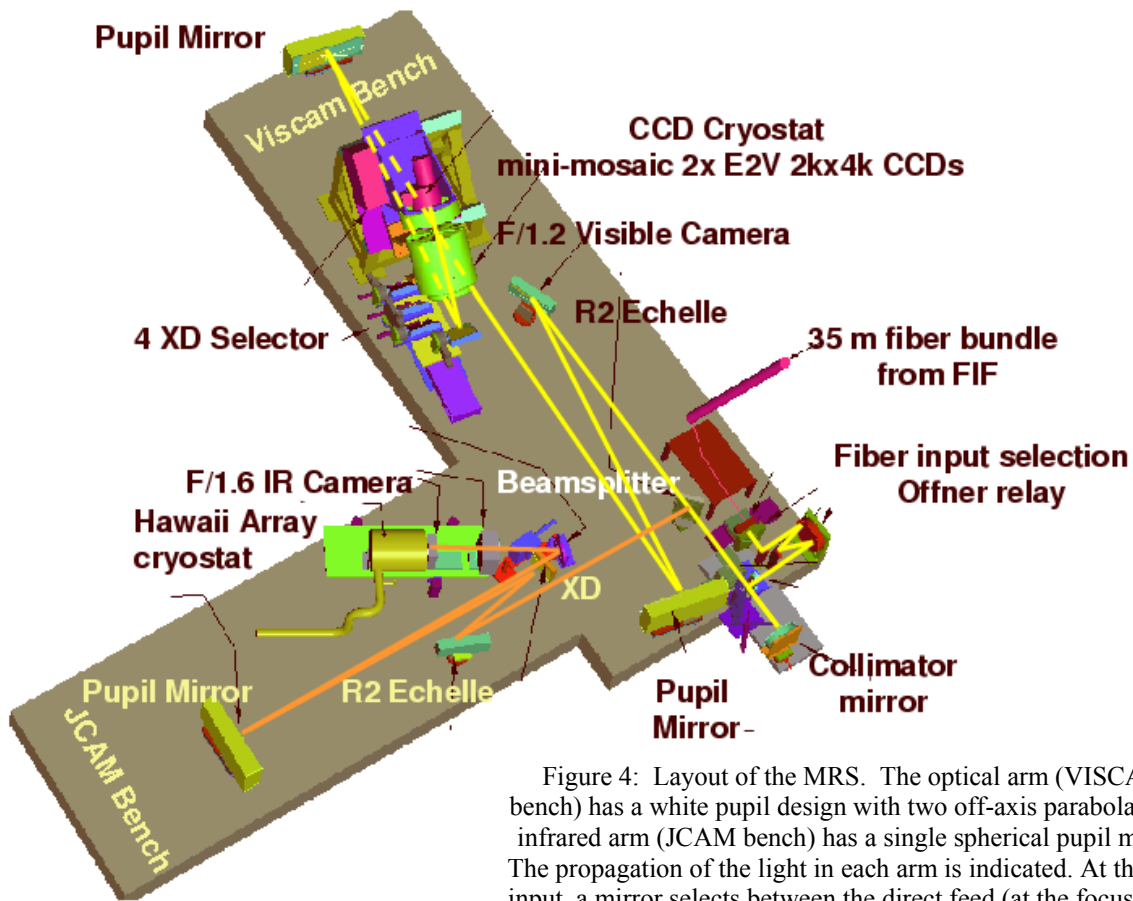


Figure 4: Layout of the MRS. The optical arm (VISCAM bench) has a white pupil design with two off-axis parabolas. The infrared arm (JCAM bench) has a single spherical pupil mirror. The propagation of the light in each arm is indicated. At the fiber input, a mirror selects between the direct feed (at the focus of the collimator) or the many other options reimaged through an Offner relay system.

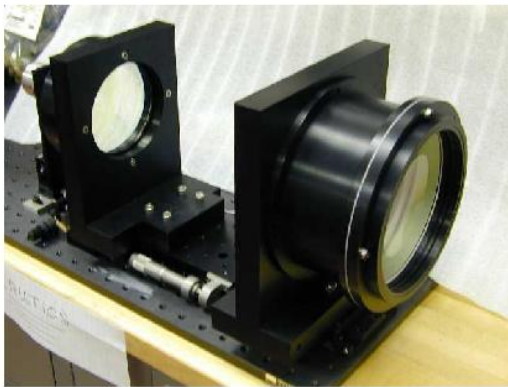
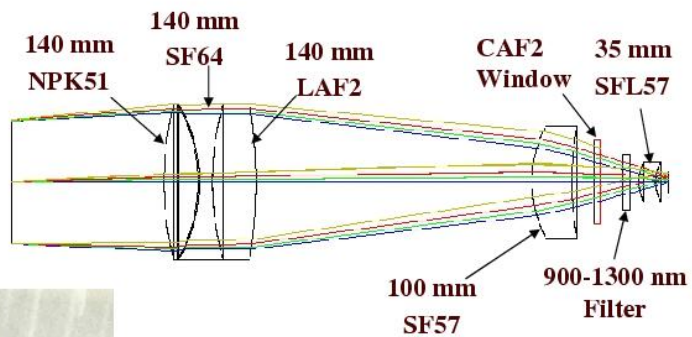
The layout of the MRS spectrograph is shown in figure 4. The MRS spectrograph has two major components, a visible beam and a red beam, fed by a common fiber and slit selection system. The visible beam is a cross-dispersed echelle white pupil system. The camera-detector system, VISCAM, is an all-refracting camera with a CCD mosaic. The NIR Beam is similarly a white pupil cross dispersed echelle spectrograph. However, the white pupil optics are different here, using a single spherical relay mirror, in an attempt to save cost while maintaining performance. The camera-detector system in the NIR beam is called JCAM as it is designed for use in the J-band spectral region. The camera is again an all refracting system. The detector is a Rockwell Scientific 1024^2 HgCdTe “Hawaii” array.

The light enters the spectrograph either from the Direct Feed (DF) where a selection of red and blue optimized fibers in each of 1.5 and 2.0 arcsec diameter are available, and are located at the focus of the collimator mirror, or through an Offner relay system. The DF is the only feed commissioned, currently. The Offner relay allows the many longslit, multi-object and IFU modes to be inserted into the beam with a deployable relay mirror. This system has a mask with a range of selectable slits at its intermediate focus, to select resolving power. From the collimator, the beam reaches the R2 Echelle. Two options are available, but it is likely that one will be chosen for long-term use. The dispersed light is then reimaged to an intermediate focus half way along the bench by an off-axis parabolic pupil mirror, and then by a second, identical, pupil mirror onto the cross-disperser. A selection of four cross-dispersers are available, to accommodate the wide range of input fiber formats. From the cross-disperser, the light is diffracted out of the plane of the optical bench and into the $f/1.2$ refractive camera. The design of the camera was made by H. Epps²³. The elements were manufactured by Coastal Optical, and the barrel design and assembly were accomplished by Alan Shier and the Pilot Group.

The infrared (JCAM) beam is split off by a dichroic beamsplitter following collimation. The IR light then encounters the R2 echelle and cross disperser, and a spherical mirror then reimages the pupil onto the camera entrance, via a fold flat. The infrared arm can be used simultaneously with the optical arm, with the DF input, and provides resolving powers of 5000 and 10000. The optical design of the camera is shown in Figure 5. Tests of the system with a J band blocking filter show good image quality, and the arm will be commissioned this year.

JCAM Camera Optics and Cell

JCAM Optical Design



L. Ramsey, 1999

Figure 5: The JCAM near-IR camera for the MRS. The design consists of a bonded triplet and a singlet, all of which are warm. Blocking of thermal emission at wavelengths beyond $1.3 \mu\text{m}$ is provided by a cold filter within the cryostat.

3.2.3 MRS CCD Detector System

The detector system is a mini-mosaic of a pair of Marconi Applied Technologies (now E2V Technologies) 2048 x 4102, 15 micron pixel CCDs. This format provides simultaneous wavelength coverage from 450 to 920 nm with the 316 groove mm^{-1} cross disperser grating. The system was supplied by GL Scientific, and like the other HET instruments, uses a CryoTigerTM cryocooler.

3.2.4 MRS Performance

Of the many potential modes of MRS, only the direct feed (DF) with 1.5 and 2 arcsec diameter fibers is commissioned, currently. This mode has been used for science observations for a trimester. The image quality of the optical system meets specifications over the entire wavelength range, and the stability of the instrument is good. The only problem is several patches of scattered light that originate within the MRS enclosure. These have appeared in the last couple of months, and will be eliminated by careful imaging of the enclosure interior with a CCD camera and through inspection with night-vision goggles. Figure 6 shows the appearance of these patches in an observation of a faint planetary nebula associated with the galaxy M101. The 30-minute observation was obtained by blind-offset of the fiber probe, and the [OIII] λ 5007 emission line is circled. The line flux is 1.1×10^{-16} erg/cm²/s.

The throughput of MRS has been measured under varying conditions of seeing against bright stars and also estimated from planetary nebula emission lines with known line fluxes. These measures indicate that with 1.5 arcsec FWHM image quality, the MRS with 1.5 arcsec diameter fibers gives a peak throughput of 3.3%, including the fiber insertion losses, and with the current HET primary mirror coating problems. Figure 7 shows the efficiency measured with the 1.5 arcsec diameter red fiber of the DF. Further improvement to the image quality, and recoating of the primary mirror, should raise the peak to close to 10% under the best conditions. When HET meets specifications, the visible beam of the MRS is expected to deliver S/N ratio ~ 100 in 1 hour at R=5,080 on V=20 stars in 1 arcsec seeing with a 2 arcsec fiber.

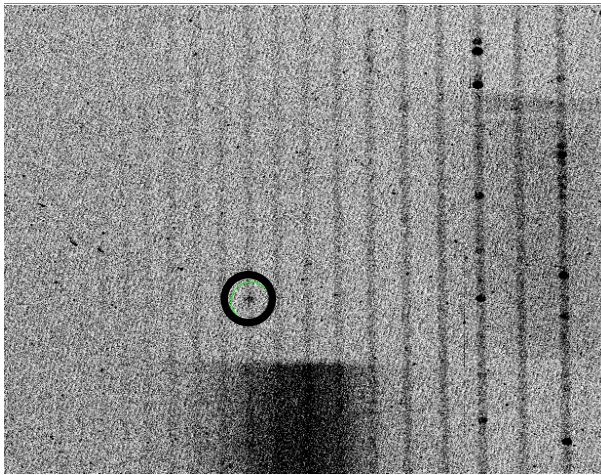


Figure 6: Example data from MRS of a planetary nebula in M101, showing part of the spectrum. The [OIII] λ 5007 emission line is circled. Scattered light of several counts is seen in several places on the detector (data courtesy of R. Ciardullo, see text).

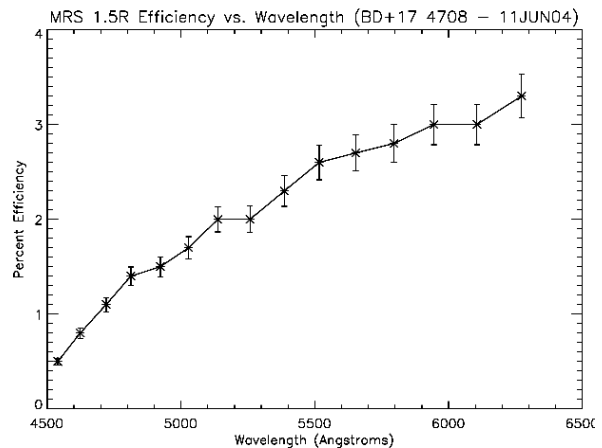


Figure 7. On-sky throughput of MRS and HET over 450-600 nm, measured to above the atmosphere for an unobstructed 8 m diameter aperture (the effective diameter of the HET). Full scale is 4%. The red 1.5 arcsec diameter fiber was used in 1.5 arcsec FWHM image quality. The strong decrease to the blue is dominated by the degraded primary mirror reflectivity.

3.3 The High Resolution Spectrograph

The HET High Resolution Spectrograph (HRS) has been described by Tull⁹, and in a previous review⁵. It is a fiber-fed, grating cross-dispersed echelle spectrometer that uses Barranne's white-pupil concept as adapted for ESO's VLT UVES by Delabre and Dekker. A refractive camera avoids a central obstruction but limits the bandwidth to 410 nm – 1.05 μ m. Light is fed from the HET with either 2 or 3 arcsecond fibers, and the choice of 0, 1, or 2 sky fibers. The 3 fibers of each of the two sizes are in a line and are separated by 10 arcseconds at their input. The output ends of these two fiber sets are mounted on a motorized stage which selects the source to be positioned at the insertion point into the spectrometer. The possible sources are the 2 arcsec fibers, the 3 arcsec fibers, the calibration feed, a prototype fiber

image slicer, a black mask, and an unobstructed path to pass a collimation laser. The $f/4$ light diverging from the output of a source fiber is collimated to a 7.5 mm diameter beam size over a 100 mm length, before being focused at $f/10$ onto the slit of the spectrometer. The collimated region is used for the filter wheel that suppresses the 2nd order of the cross disperser, for an insertable temperature-stabilized I_2 gas absorption cell, and for an aperture stop at the pupil position which is available when the I_2 cell is retracted. The spectrometer slit mechanism selects one of 12 slits of different widths and lengths that are etched in a metal foil. Resolving powers of 15,000, 30,000, 60,000, and 120,000 are available via a choice of 4 different widths, and the number of sky fibers passed by a given slit is determined by its length. A pinhole that images to 2 CCD pixels ($R=120,000$) is also on the slit mask. Two cross dispersers are available, each being kinematically mountable at any one of 10 different angles of incidence. The 316 groove mm^{-1} grating gives 400 nm of coverage, with the central wavelength changing in 100 nm steps. The 600 groove mm^{-1} grating gives 200 nm of coverage, with the central wavelength changing in 50 nm steps.

The CCD system is a mosaic of two Marconi Applied Technologies (now E2V Technologies) 2048 x 4102, 15 micron pixel CCDs. It is controlled by a McDonald Observatory Version 2 CCD controller. One amplifier is used per CCD, and they run simultaneously at 100 kpixels per second per amplifier. 18-bit digitization at 0.68 electrons per ADU resolves well the 2.8 electron readout noise while fully spanning the 180,000 electron full well. A CryoTiger cryocooler system is used for cooling the mosaic, and the vacuum is maintained with a 175 cm^3 activated charcoal cryopump, a custom Varian 2 L s^{-1} noble-diode ion pump, and a Pfeiffer Full-Range vacuum gauge. The pump and gauge are only run during the day due to their light emissions, and the vacuum is 2×10^{-7} mbar or better. The system stays cold typically for six or more months at a time, dictated by occasional warm-ups for HET engineering activities.

The CCDs are oriented such that the columns are parallel to the echelle dispersion dimension, so that the 72-pixel gap between the two CCDs takes out approximately one order rather than the center of all the orders. At $R=15,000$ and $R=30,000$, the recommended binning corresponds to about 3 pixels per resolution element, at $R=60,000$ it corresponds to either 2 or 4 pixels per resolution element, and at $R=120,000$ the only choice is 2 pixels per resolution element. The one significant issue is the cosmetic quality of the CCD that covers the red part of the spectrum. While given a grade-1 designation, it has many bright defects, and the charge transfer efficiency is bi-modal depending upon which region of columns is considered. It will be replaced this year.

Calibration light does not come down the fibers from the telescope, but rather enters the HRS through a fiber bundle from each of a Th-Ar and flat field lamp outside the HRS enclosure. Within the calibration head on the HRS source selector, the light from the lamp in use diverges out of the fiber bundle over a 20 mm length, passes through a diffuser, and on to an exit slit about 10 mm away. That slit is slightly larger than the widest and longest spectrometer slit, so that all possible spectrometer slits are uniformly illuminated. The aperture stop in the collimated space limits the focal ratio to $f/4$ to match that of the telescope fibers.

The HRS offers a considerable number of possible configurations, most of which are appropriate for observations of one type or another. Full details of the HRS configurations and restrictions are available by following the HRS links from the HET web site at <http://het.as.utexas.edu/HET/hetweb/>. In particular, order overlap places restrictions on the number of sky fibers that can be used at bluer wavelengths with 316 groove mm^{-1} cross disperser.

3.3.1 Radial Velocity Precision

The HRS is delivering outstanding radial velocity precision for programs using the I_2 absorption cell at $R=60,000$. The HET planet search programs of Cochran and Endl²⁴ are receiving significant allocations of time, and the queue-scheduling of HET is particularly effective for these programs. Back-to-back velocity measurements of stars in these programs generally agree to within a few tenths of one metre per second. Sources of error include the intrinsic velocity performance of the HRS, the signal-to-noise ratio of the data, intrinsic stellar sources of velocity “jitter”, and analysis imperfections. Figure 8 shows histograms of the rms velocity precision obtained for all stars in the programs and for the survey of fainter M dwarfs. For 173 stars in the full sample with $V=6-10$, the best precision is in the range of $\sigma=1-3$ m/s, and a significant number have $\sigma=1$ m/s. The majority have precision better than 10 m/s. For the fainter M dwarfs with $V=9-12$, the majority are better than 15 m/s. The first planet discovered entirely by HET is companion to the metal-rich K0V star HD37605, and has an orbital period of 54.23 days, an orbital eccentricity of 0.737, and a minimum mass of 2.84 Jupiter masses²⁴. The queue-scheduled operation of the Hobby-Eberly Telescope enabled the discovery of this relatively short-period, but high eccentricity planet with a total observation time span of just two orbital periods.

3.3.2 Current performance

The HRS saw first light in April 2001 and entered routine queue scheduled observing in late May 2001. It has observed objects from 1st to 18th magnitude, at signal-to-noise ratios between 5:1 and 1000:1, and at flux levels comparable to the sky flux through the fibers. Very high signal-to-noise ratios have been reported²⁵ in close agreement with those expected from the detected signal level. The resolution and image shapes across the field from the R=120,000 pinhole are in very close agreement with ray-tracing. The HRS is giving excellent data quality and stability, but its competitiveness is significantly reduced by the poor throughput of the HET/HRS combination. Improvements to the reflectivity of the HET primary mirror will increase the telescope throughput by a factor of two. The poor HET image quality has required the use of large fibers to capture a significant fraction of the object flux. Those fibers are very inefficiently coupled into the available inter-order space of the HRS, and also capture a large amount of sky flux, brightening the sky-noise limiting magnitude considerably. The improving HET image quality, and improved setup and guiding accuracy, have yielded improved coupling into the fiber at the telescope end. We will install new 1.5 arcsec. diameter Polymicro FBP fibers, and implement image slicing for some modes, in order to improve coupling from the output of the fibers into the HRS, for the instrument to reach its full potential.

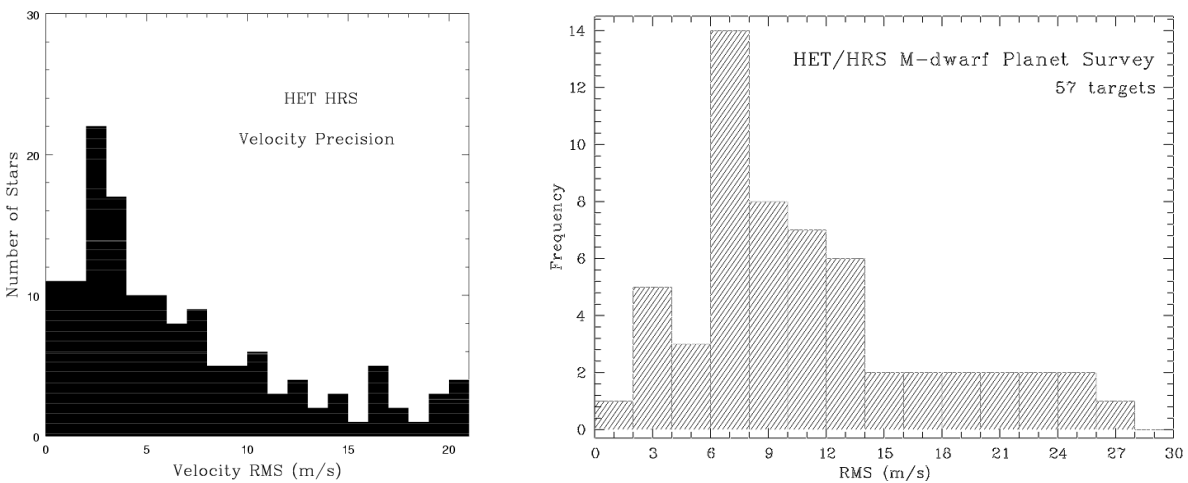


Figure 8: Histograms presenting the radial velocity precision achieved by HRS for the HET planet search programs. The left panel presents the results for 173 stars of type late F to K with $V=6-10$ in the main program. Many of these stars have velocity rms of 1-3 m/s, with the majority better than 10 m/s. The right panel shows the results for 57 M dwarfs with fainter magnitudes, $V=9-12$, where the best precision is around 8 m/s and most are better than 15 m/s rms.

4. HET NEAR-INFRARED CAPABILITY

In addition to the infrared arm of the MRS (section 3.2), we are developing an infrared extension for the LRS, called LRS-J^{26,27,28}. The instrument and status are described in detail in these proceedings²⁸. LRS-J is a cryogenic camera that replaces the optical camera of the LRS, providing coverage from 900 to 1300 nm. The primary aim of the project is to provide multi-object near-IR spectroscopic capability, using the existing LRS capability, without constructing a new instrument. The space and payload constraints of the HET prime focus instrument package would make a new instrument impossible. Space constraints make it necessary that the swap be a manual replacement, but this can be achieved with minimal down-time. As a result, we will deploy LRS-J in blocks of time, several times per year. The wavelength coverage is achieved at resolving power $R\sim 2000$, with the 1.3 arcsec wide slitlets of the LRS MOS unit, in two exposures. This is sufficient to provide good subtraction of the OH⁺ sky emission lines. Two volume phase holographic gratings^{22,26} replace the optical gratings to provide this coverage. VPH gratings were the only way to achieve the dispersion and exact wavelength coverage desired, while maintaining high efficiency. The 170 mm diameter VPH gratings are among the largest deployed and were manufactured by Wasatch Photonics. They are sandwiched between

large prisms of SFL57 to steer the light on-axis. The Rockwell Scientific Hawaii-IRG detector will be controlled by the same CCD controller that reads out the LRS optical camera CCD²⁷.

LRS-J is an f/1 140 mm catadioptric camera²⁶, which is a challenging system for cryogenic use. A cold blocking filter rejects thermal background from the warm spectrograph, assisted by a Schott PK50 glass field flattener lens, which cuts off around 2.35 μm . We will complete testing of LRS-J in the autumn of 2004 and have first light before the end of the year.

5. SUMMARY AND FUTURE WORK

The HET has not yet achieved its specified performance in terms of image quality and throughput, but we have demonstrated that the telescope will meet specifications by delivering 0.8 arcsec. FWHM images for extended periods. Re-coating of the primary mirror with aluminum will double throughput and cut the large scattered light background that is limiting faint observations. All the instruments themselves have high throughputs close to predictions, so once the HET throughput is improved, we can expect the instrumentation to perform very well. We also look forward to the LRS-J and MRS IR arm entering science operations, which will provide new capabilities. In the longer term, it is evident that for HET to have a string survey niche, it needs a wider field of view and we are designing a new corrector with a target of 20 arcmin. diameter field. This will provide a powerful multiplex advantage, and will allow us to use wavefront sensing to keep alignment of the corrector during a track, but providing access to a sufficient number of bright stars. We are also developing the design of a highly multiplexed integral field spectrograph for use with the new corrector, that will be capable of observing 29 sq. arcminutes at a time with 1 sq. arcsec resolution on the sky and coverage from 340-570 nm simultaneously. This instrument is called VIRUS and is described in these proceedings²⁹.

ACKNOWLEDGEMENTS

Special thanks go to John Good, Joe Tufts, Bob Tull, Leland Engel, and Marsha Wolf for their contributions to the HET facility instruments described here. John Booth leads the HET improvement project. We thank the HET operations staff, the McDonald Observatory engineering and operations staff, and particularly Jim Fowler, Gordon Wesley, and Sam Odoms for their extraordinary efforts in getting HET to its present state of operations. Robin Ciardullo, Bill Cochran, and Mike Endl provided figures. George Trammell, Robin Ciardullo, and Don Schneider contributed a MRS throughput analysis.

The Marcario Low Resolution Spectrograph is a joint project of the Hobby - Eberly Telescope partnership and the Instituto de Astronomía de la Universidad Nacional Autónoma de México (IAUNAM). Construction of the HET HRS was funded by NSF Grant AST-9531674, by supplemental funds under NASA Grant NAGW-1477, and by a legislative appropriation from the State of Texas, further supplemented by McDonald Observatory funds. Construction of HET MRS has also been supported by the NSF.

REFERENCES

1. G. J. Hill, 1995, "Science with the Hobby-Eberly Spectroscopic Survey Telescope," in *Wide Field Spectroscopy*, S.J. Maddox & A. Aragon-Salamanca eds., World Scientific, Singapore, pp. 49-54.
2. J.A. Booth, M.J. Wolf, J.R. Fowler, M.T. Adams, J.M. Good, P.W. Kelton, E.S. Barker, P. Palunas, F.N. Bash, L.W. Ramsey, G.J. Hill, P.J. MacQueen, M.E. Cornell, & E.L. Robinson, "The Hobby-Eberly Telescope Completion Project", in *Large Ground-Based Telescopes*, Proc SPIE **4837**, paper 109, 2002
3. J.A. Booth, *et al.* "The Hobby-Eberly Telescope: performance upgrades, status and plans," Proc. SPIE, **5489**, paper 18, 2004
4. G. J. Hill, "The Hobby Eberly Telescope : Instrumentation and Current Performance," in *Optical and IR Telescope Instrumentation and Detectors*, Proc. SPIE **4008**, 50, 2000.
5. G.J. Hill, P.J. MacQueen, & L.W. Ramsey, "Performance of the facility instruments on the Hobby-Eberly telescope," Proc. SPIE, **4841**, 43, 2003.
6. Hill, G. J., Nicklas, H., MacQueen, P. J., Tejada de V., C., Cobos D., F. J., and Mitsch, W., 1998, "The Hobby-Eberly Telescope Low Resolution Spectrograph", in *Optical Astronomical Instrumentation*, S. D'Odorico, Ed., Proc. SPIE **3355**, 375.

7. Hill, G. J., Nicklas, H., MacQueen, P. J., Mitsch, W., Wellem, W., Altmann, W., and Wesley, G. L., 1998, "The Hobby-Eberly Telescope Low Resolution Spectrograph: Mechanical Design", in *Optical Astronomical Instrumentation*, S. D'Odorico, Ed., Proc. SPIE **3355**, 433.
8. F. J. Cobos D, C. Tejada de V., G. J. Hill, and F. Perez G., 1998, "Hobby-Eberly Telescope low resolution spectrograph: optical design," in *Optical Astronomical Instrumentation, Proc. SPIE 3355*, 424.
9. R. G. Tull, 1998, "High-resolution fiber-coupled spectrograph of the Hobby-Eberly Telescope," in *Optical Astronomical Instrumentation, Proc. SPIE 3355*, 387.
10. S. D. Horner and L. W. Ramsey, 1998, "Hobby Eberly Telescope medium-resolution spectrograph and fiber instrument feed," in *Optical Astronomical Instrumentation, Proc. SPIE 3355*, 399.
11. L.W. Ramsey, L.G. Engel, N. Sessions, C. de Filippo, M. Graver, & J. Mader, "The Hobby-Eberly Telescope medium resolution *spectrograph and fiber instrument feed*", in *Instrument Design and Performance for Optical/Infrared Ground-Based Telescopes, Proc SPIE 4841*, 1036, 2003
12. R. K. Jungquist, 1999, "Optical design of the Hobby-Eberly Telescope four-mirror spherical aberration corrector," in *Current Developments in Optical Design and Optical Engineering, Proc. SPIE 3779*, 2.
13. V.L. Krabbendam, T.A. Sebring, F.B. Ray & J.R. Fowler, 1998, "Development and performance of Hobby-Eberly Telescope 11-m segmented mirror," in *Advanced Technology Optical/IR Telescopes VI, Proc. SPIE 3352*, 436.
14. J. A. Booth, F. B. Ray, and D. S. Porter, 1998, "Development of a star tracker for the Hobby Eberly Telescope", in *Telescope Control Systems III, Proc. SPIE 3351*, 298.
15. K. Meiring & D.H. Buckley, "The Southern African large Telescope (SALT) Project: progress and status after 4 years," Proc. SPIE, **5489**, paper 41, 2004.
16. M.J. Wolf, M. Ward, J.A. Booth, B. Roman, "Polarization shearing laser interferometer for aligning segmented telescope mirrors," in *Large Ground-Based Telescopes, Proc SPIE 4837*, paper 88, 2002
17. M.J. Wolf, M. Ward, J.A. Booth, A. Wirth, G.L. Wesley, D. O'Donoghue, & L. Ramsey, "Mirror Alignment Recovery System on the Hobby-Eberly Telescope", in *Large Ground-Based Telescopes, Proc SPIE 4837*, paper 82, 2002
18. P. Palunas, J.R. Fowler, J.A. Booth, G. Ames, G. Damm, "Control of the Hobby-Eberly Telescope primary mirror array with the segment alignment maintenance system," Proc. SPIE, **5496**, paper 84, 2004.
19. J.M. Good, P.W. Kelton, J.A. Booth, E.S. Barker, "Hobby-Eberly Telescope Natural Ventilation System Upgrade", in *Large Ground-Based Telescopes, Proc SPIE 4837*, paper 26, 2002
20. J.D. Wolfe, D.M. Sanders, S. Bryan, N.L. Thomas, "Deposition of durable wide-band silver mirror coatings using long-throw, low-pressure, DC-pulsed magnetron sputtering", Proc. SPIE, **4842**, 343, 2003
21. M.J. Wolf, G.J. Hill, W. Mitsch, F.V. Hessmann, W. Altmann, and K.L. Thompson, 2000, "Multi-object Spectroscopy on the Hobby-Eberly Telescope Low Resolution Spectrograph," in *Optical and IR Telescope Instrumentation and Detectors, Proc. SPIE 4008*, 216, 2000
22. G.J. Hill, M.J. Wolf, J.R. Tufts, & E.C. Smith, "Volume Phase Holographic (VPH) Grisms for Optical and Infrared Spectrographs", in *Specialized Optical Developments in Astronomy, Proc. SPIE 4842*, paper 05, 2002.
23. H.W. Epps, "Development of large high-performance lenses for astronomical spectrographs," Proc. SPIE, **3355**, 111, 1998
24. W. D. Cochran, *et al.*, "The First HET Planet: A Companion to HD 37605," ApJ letters, in press, 2004 (astro-ph/0407146)
25. Allende Prieto, C., Lambert, D.L., Tull, R.G., and MacQueen, P.J., "Convective wavelength shifts in the spectra of late-type stars", 2002, ApJ, **566**, L93.
26. C. Tejada, G.J. Hill, & F.J. Cobos, "Design of an f/1 camera for the HET low-resolution spectrograph IR extension," Proc. SPIE, **4841**, 1407, 2003
27. J.R. Tufts, G.J. Hill, P.J. MacQueen, & M.J. Wolf, "LRS-J: Instrument design and characterization," Proc. SPIE, **5492**, paper 52, 2004
28. J.R. Tufts, P.J. MacQueen, & G.J. Hill, "Hobby-Eberly telescope: LRS-J HAWAII-1 detector electronics," Proc. SPIE, **4841**, 667, 2003
29. G.J. Hill, P.J. MacQueen, C. Tejada, P.J. Cobos, P. Palunas, K. Gebhardt, & N. Drory, "VIRUS: a massively-replicated IFU spectrograph for HET," Proc. SPIE, **5492**, 25, 2004